

## Critical Casimir Effect near the $^3\text{He}$ - $^4\text{He}$ Tricritical Point

R. Garcia and M. H. W. Chan

*Department of Physics, The Pennsylvania State University, University Park, Pennsylvania 16802*

(Received 12 September 2001; published 6 February 2002)

We present capacitance measurements of the equilibrium thickness of  $^3\text{He}$ - $^4\text{He}$  mixture films as a function of temperature and concentration. The films are adsorbed on a Cu substrate situated above bulk liquid mixture. As we scan across the tricritical point, we observe a thickening of the film indicating the presence of a repulsive critical Casimir force.

DOI: 10.1103/PhysRevLett.88.086101

PACS numbers: 68.35.Rh, 64.60.Fr, 67.40.Kh, 67.70.+n

One of the most beautiful aspects of physics is how phenomena in widely different systems are described by the same mathematical formulation. In electromagnetism, the Casimir force is due to the confinement of zero-point electromagnetic fluctuations between two plates a finite distance apart [1]. In a completely analogous way, the confinement of critical fluctuations in an adsorbed film leads to a thickness dependent correction to the free energy of the film and, therefore, a critical Casimir force between the interfaces of the film [2–8]. Measurements of the thickness of  $^4\text{He}$  films adsorbed on Cu substrates have confirmed the existence of the critical Casimir effect near the superfluid transition [9,10]. The force is observed to be attractive, producing a dip in the film thickness centered just below  $T_\lambda$ . Additional evidence of the critical Casimir effect has been reported also in binary fluid films [11]. However, in this case there is very significant quantitative disagreement with theoretical predictions, possibly related to the nonwet state of the films [7,11].

The tricritical point in  $^3\text{He}$ - $^4\text{He}$  mixtures provides another system for measuring the critical Casimir effect [3–5,7,8]. The tricritical point (TP) in Fig. 1(a) is the point in the bulk mixture phase diagram where the line of superfluid transitions terminates at the top of the coexistence region [12]. As we approach TP, this system is predicted to exhibit an attractive Casimir force for symmetric order parameter boundary conditions and a repulsive force for nonsymmetric boundary conditions [4,7,8]. Our capacitance measurements of the thickness of adsorbed films near TP is consistent with the presence of a repulsive force. A preliminary report on this effect has been published previously [13].

The experimental cell we use, shown schematically in Fig. 1(b), has two capacitors. The electrodes of the capacitors are 1.7 cm diameter coin-shaped Cu disks epoxied into annular Cu electrical guard rings. The spacing between the plates is maintained by 0.2 mm thick Cu spacers inserted between the guard rings. Capacitor B, submerged in bulk liquid, is used to measure the bulk liquid's dielectric constant  $\epsilon_B$  and to determine the phase separation temperature for each bulk liquid concentration. The films are adsorbed onto the electrode surfaces of capacitor F, situated above the bulk liquid. Capacitor F is the same as capacitor 5 of

Ref. [9], whose highly polished surfaces were determined to be reasonably free of scratches and other defects. The cell hangs from a temperature-regulated ballast, with no heat applied directly to the cell. This arrangement results in a temperature noise at the cell of less than 2  $\mu\text{K}$ . The equilibration time is about 1 h.

At the start of each experimental run, we admit into the cell appropriate amounts  $n_3$  of  $^3\text{He}$  and  $n_4$  of  $^4\text{He}$  to obtain the desired  $^3\text{He}$  mole fraction in the bulk liquid  $X = n_3/(n_3 + n_4)$  and to maintain the liquid at a height  $2.0 \pm 0.05$  mm below capacitor F. We are able to estimate  $X$  simply from the amounts dosed into the cell since the vapor and film together comprise less than 0.2% of the total helium. We measure capacitances using a standard bridge technique [14] with reference capacitors anchored on the outside of the cell. Intermittent shifts in capacitance of as much as 2 ppm, most likely related to the release of mechanical stresses, occur throughout the course of the experiments. The effective dielectric constants  $\epsilon_B$  for capacitor B and  $\epsilon_F$  for capacitor F are calculated using  $\epsilon = C/C_o$ , where  $C$  is the capacitance and  $C_o$  is the empty capacitance measured after all the helium is pumped out. For each  $X$ , a kink in  $\epsilon_B$  signaling the onset of phase separation in the bulk liquid is used to determine the phase separation temperature  $T_{\text{sep}}$ . These  $T_{\text{sep}}(X)$  agree with those of Ref. [12], confirming the accuracy of our temperature scale. From our data, TP is located at  $X_t = 0.672 \pm 0.001$ ,  $T_t = 0.8698 \pm 0.0001$  K.

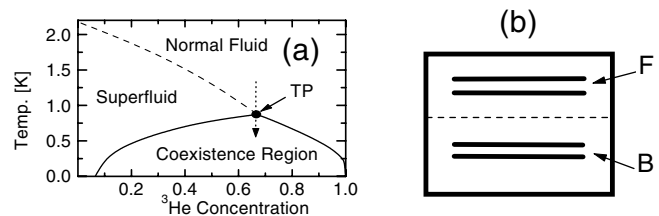


FIG. 1. (a) Phase diagram of bulk  $^3\text{He}$ - $^4\text{He}$  mixture showing superfluid transition line (dashed line), coexistence boundary (solid line), and the tricritical point (TP). The dotted arrow shows the experimental path passing through TP. (b) Schematic of the experimental cell. Capacitor B is submerged in the bulk liquid. Capacitor F is 2.0 mm above the liquid level (dashed line).

In Fig. 2, we show the expected  $^3\text{He}$  mole fraction in the film  $X_{\text{film}}$  at 1 K and at  $T_t$  as a function of the distance from the substrate  $z$ .  $X_{\text{film}}(z)$  determines the film's average density and its effective dielectric constant  $\bar{\epsilon}_{\text{film}}(X, T)$ . The profiles are calculated using the numerical method of Ref. [15] and the concentration susceptibility data of Ref. [16] for an adsorbed film 500 Å thick and with the bulk liquid near the tricritical concentration. The enrichment of the  $^4\text{He}$  near the substrate is due entirely to the substrate's van der Waals force and the different molar volume of the isotopes due to quantum zero-point motion. The effect of gravity is negligible. As we approach  $T_t$ , the  $^4\text{He}$  rich layer near the substrate expands due to the diverging concentration susceptibility, yielding a 0.5% increase in the average film density. The fact that this increase is small is important for the interpretation of our  $\epsilon_F$  data.

In Fig. 3(a), we show the result of a typical measurement of  $\epsilon_F$  as a function of  $T$  when  $X \approx X_t$ . The data, including the bump centered at 0.848 K, are reproducible on cooling and warming. In our system, the helium film adsorbed on the capacitor plates contributes  $\sim 2.7 \times 10^{-5}$  to  $\epsilon_F$  while the vapor between the plates contributes  $\sim 5.6 \times 10^{-5}$ . While most of the temperature dependence in  $\epsilon_F$  in Fig. 3(a) is accounted for by the temperature dependence of the saturated vapor density, the absence of a comparable peak in the vapor density near  $T_t$  [16] implies the observed bump is due to either a thickening of the adsorbed film or an increase in the film density. However, the 0.5% increase in the film density as we approach  $T_t$ , noted above, can account for at most 6% of the observed anomaly.

In Fig. 3(b) we show the film thickness  $d$  calculated from the data of Fig. 3(a). The main result of this Letter is the asymmetric 90 Å peak in the film thickness centered below  $T_t$ . Ideally, to calculate  $d$  from  $\epsilon_F$ , we use

$$d = \frac{1}{2}G(1/\epsilon_F - 1/\bar{\epsilon}_{\text{film}})/(1/\epsilon_{\text{vapor}} - 1/\bar{\epsilon}_{\text{film}}), \quad (1)$$

where  $G$  is the gap between the capacitor plates [9]. Adding in series the capacitances for each layer of the film, we obtain the effective dielectric constant of the film  $\bar{\epsilon}_{\text{film}}(X, T) = d[\int_0^d dz/\epsilon(z)]^{-1}$ , where  $\epsilon(z)$  is the dielectric constant corresponding to  $X_{\text{film}}(z)$ . In our calculations, we have made the approximation that  $\bar{\epsilon}_{\text{film}}(X, T)$  is independent of  $T$  and equal to  $\epsilon_B(X)$  at

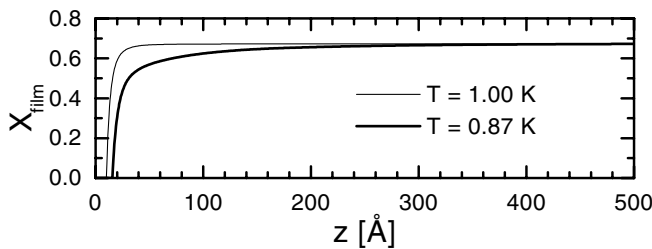


FIG. 2.  $^3\text{He}$  mole fraction in the film  $X_{\text{film}}$  calculated as a function of distance from the substrate surface  $z$  at 1 K and at  $T_t$ .

$T = 1$  K. Based on the concentration gradient profiles in Fig. 2, this approximation introduces at most a 5 Å error in the calculated  $d$ . The dielectric constant of the vapor  $\epsilon_{\text{vapor}}(X, T)$  is estimated from the vapor density using the Clausius-Mossotti relation [17]. The vapor density, in turn, is calculated from the pressure data of Ref. [16]. While a second virial coefficient correction is included in calculating the vapor density, the size of this correction is comparable to the uncertainty in the various calibrations. From previous experiments [9,10], we know that the capacitive technique accurately measures the change in  $d$ , while the absolute value of  $d$  is more susceptible to errors due to capacitance calibrations, scratches on the surface, and uncertainty in the vapor pressure corrections. In this experiment we estimate that the uncertainty in the absolute value of  $d$  due to these sources of error is about 20%.

Near TP, the thickness of a mixture film wetting a Cu substrate a height  $h$  above the bulk liquid is given by

$$Mgh = \alpha/d^3 + Vk_B T_t \vartheta/d^3, \quad (2)$$

a result that can be derived using the Gibbs-Duhem relation [18]. In the first term,  $g$  is the gravitational acceleration,  $h$  is the height above the bulk liquid, and  $M$  is the average mass per atom of the bulk mixture. In the second term,  $\alpha = 2600 \text{ K Å}^3/(1 + d/193 \text{ Å})$  is a coefficient characterizing the attraction of the helium atom to the Cu substrate [19]. The last term is the predicted chemical potential difference between the film and bulk due to the critical Casimir force [2,3,5,9], where  $k_B$  is Boltzmann's

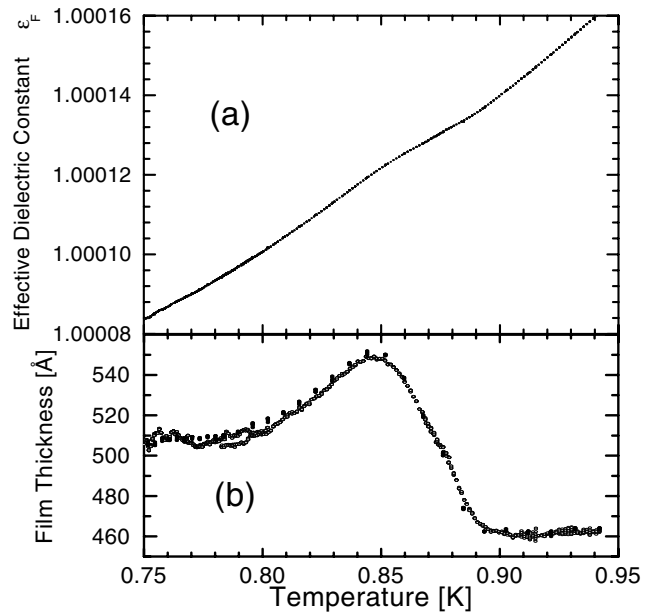


FIG. 3. (a) Effective dielectric constant  $\epsilon_F$  for capacitor F as a function of temperature for  $X \approx X_t$ . (b) Mixture film thickness calculated from data of panel (a), showing a 90 Å peak in  $d$  at  $T \approx 0.848$  K. The open and closed circles are two separate runs.

constant,  $T_t$  is the tricritical temperature,  $V$  is the specific volume per atom in the bulk liquid [20], and  $\vartheta$  is a dimensionless scaling function predicted to be a function of  $d/\xi$  [5,9,21], where the correlation length  $\xi$  depends on  $X$  and  $T$ . The most important aspect of Eq. (2) is that  $V$  and  $M$ , which depend on  $X$ , are properties of the *bulk liquid* and  $\alpha$  is the same for  $^3\text{He}$  and  $^4\text{He}$  [19] so that concentration gradients in the film do not affect the equilibrium film thickness  $d$ . In the present case, for  $h = 2.0$  mm and  $X = 0.672$ , we expect  $d \approx 460$  Å.

In Figs. 4(a) and 4(b) we show  $d$  calculated from the measured  $\epsilon_F$  for  $X \geq X_t$  and for  $X \leq X_t$ , respectively. For easy comparison, the data have been shifted vertically so that the film thickness at  $T \sim 1$  K equals  $d$  predicted from Eq. (2) without the last term due to the Casimir force. These shifts are within the 20% uncertainty in the absolute value of  $d$  noted above. The tricritical curve  $X \sim X_t$  provides a common reference for both figures. In Fig. 4(a), as  $X$  increases past  $X_t$ , the film thickness profile begins to deviate from the tricritical curve at a temperature slightly below  $T_{\text{sep}}$ , with a sharp drop away from the tricritical curve occurring precisely at  $T_{\text{sep}}$  (marked with a thin arrow). For  $X = 0.718$ , there is only a 40 Å steplike increase in  $d$  at  $T_{\text{sep}}$ . In Fig. 4(b) for  $X$  below  $X_t$ , we note the film thickness profiles are different above and below  $X \sim 0.6$ . For  $X > 0.6$ , the various curves approximately collapse onto

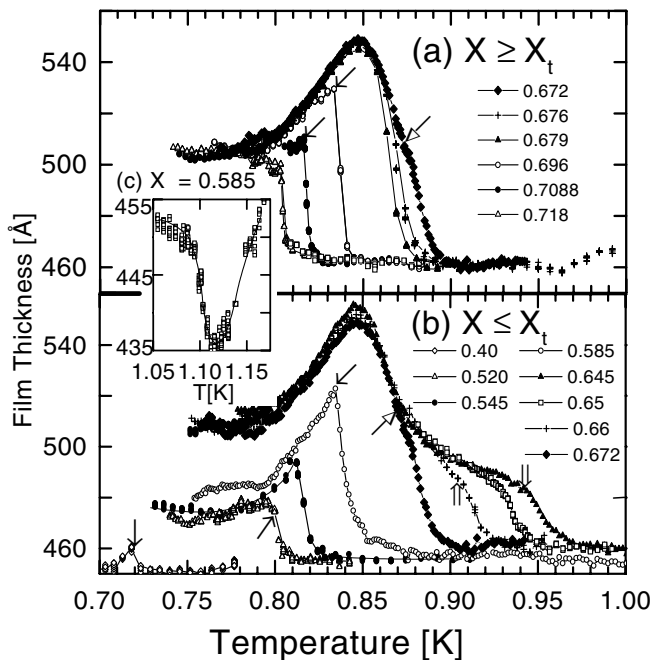


FIG. 4. (a) Film thickness calculated from  $\epsilon_F$  for  $X \geq X_t$ . For some curves, thin arrows indicate the point where the bulk liquid phase separates. The arrow with the large head indicates the tricritical point. (b) Film thickness for  $X \leq X_t$ . For some curves, arrows with double lines show the superfluid onset temperature based on Refs. [12] and [16]. (c) A blowup for  $X = 0.585$  near 1.10 K showing a dip near the bulk superfluid transition in contrast to the shoulder for  $X > 0.6$ .

the tricritical curve below  $T_t$ . Above  $T_t$ , a steplike shoulder is found near the bulk superfluid transition temperature for each  $X$  (marked by arrows with two lines) [12,16]. This steplike thickening of the film upon decreasing the temperature through the bulk superfluid transition temperature is in strong contrast to the thinning or dip observed in more dilute mixtures and pure  $^4\text{He}$  [9]. Figure 4(c) shows that such a dip still appears to be present for a mixture film with  $X = 0.585$ . For  $X < 0.6$ , the curves near 0.84 K and below no longer appear to collapse onto the tricritical curve. We are not certain whether this is related to the concomitant change in behavior near the superfluid transition near  $X \sim 0.6$ . The size of the peak at  $T_{\text{sep}}$  decreases as  $X$  is decreased below  $X_t$ . For  $X = 0.40$ , only a small  $\sim 10$  Å peak remains. A similar size peak in  $d$  at  $T_{\text{sep}}$  for  $X = 0.40$  has been seen in a quartz microbalance study of mixture films adsorbed on Cs [22]. While mixture films exhibit wetting transitions on Cs, for  $X = 0.40$  near  $T_{\text{sep}}$ , the experimental situation is similar to helium on Cu, namely, the film completely wets Cs.

The difference in behavior at the superfluid transition above and below  $X \sim 0.6$  is likely due to a change in the  $^4\text{He}$  rich layer close to the substrate. This layer remains superfluid above the superfluid transition temperature of the bulk mixture for  $X \geq 0.6$ , but not for  $X \leq 0.6$  [15,22]. For  $X \geq 0.6$ , this means the order parameter vanishes at the vapor interface but remains nonzero near the substrate. For such boundary conditions, the critical Casimir force at the superfluid transition is predicted to be repulsive [4,7,8]. For  $X \leq 0.6$ , the order parameter vanishes at both interfaces, just as for pure  $^4\text{He}$ , causing an attractive force. Further experiments are needed to understand how the curves change as  $X$  is varied through 0.6.

In summary, we find a thickening of the adsorbed film near TP. This peak in  $d$  is not explainable by the diverging susceptibility near TP or by any other mechanism other than a repulsive critical Casimir force [3–8]. In Fig. 5 we show  $\vartheta$  calculated from the data of Fig. 4 using Eq. (2), plotted against the scaling variable  $x = td^{1/\nu} = (\xi_o d/\xi)^{1/\nu}$ , where  $\xi_o$  is the  $X$ -dependent correlation length amplitude,  $t = T/T_t - 1$ , and  $\nu = 1$  along a constant  $X$  path [24]. We find  $\vartheta = 8.4 \pm 1.7$  at TP, the

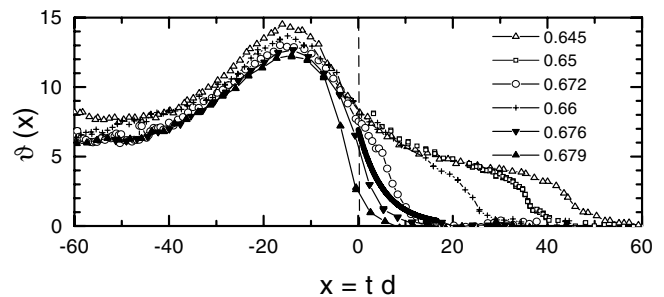


FIG. 5. The scaling function  $\vartheta$  vs scaling variable  $x$  for various  $X$  close to  $X_t$ .  $\vartheta(0) = 8.4 \pm 1.7$ . The solid line is a theoretical prediction for  $X = X_t$  [23].

uncertainty quoted being due to the 20% uncertainty in the absolute film thickness. The thick line in Fig. 5 shows a recent theoretical calculation of  $\vartheta$  for the Ginzburg-Landau XY model near the tricritical point, where the order parameter is assumed to be zero at one interface and nonzero at the other [23]. The correlation length amplitude  $\xi_o$  is an adjustable parameter. Since we do not know of any experiment measuring  $\xi_o$  above  $T_t$ , we used 1.3 Å, the value measured for concentration fluctuations below  $T_t$  in the superfluid phase [24]. The magnitude of the theoretical function, with  $\xi_o$  between 1.0 and 1.5, is in reasonable agreement with the measured  $\vartheta$ . However, there is a distinct difference between the experimental and the theoretical curve just above  $x = 0$ .

We thank H. Meyer for providing unpublished pressure data used in our calculations and M. Krech for providing the theoretical scaling function ahead of publication. We also thank M. Cole, K. Knorr, and N. Mulders for informative discussions. This work was supported by NASA's Office of Biological and Physical Research under NAG8-1761.

- 
- [1] H. B. G. Casimir, Proc. K. Ned. Akad. Wet. **51**, 793 (1948); S. K. Lamoreaux, Phys. Rev. Lett. **78**, 5 (1997); U. Mohideen and A. Roy, Phys. Rev. Lett. **81**, 4549 (1998).
- [2] M. E. Fisher and P.-G. de Gennes, C. R. Acad. Sci. Paris, Ser. B **287**, 209 (1978).
- [3] M. P. Nightingale and J. O. Indekeu, Phys. Rev. Lett. **54**, 1824 (1985); J. O. Indekeu, M. P. Nightingale, and W. V. Wang, Phys. Rev. B **34**, 330 (1986); K. K. Mon and M. P. Nightingale, Phys. Rev. B **35**, 3560 (1987).
- [4] J. O. Indekeu, J. Chem. Soc. Faraday Trans. 2 **82**, 1835 (1986).
- [5] M. Krech and S. Dietrich, Phys. Rev. Lett. **66**, 345 (1991); **67**, 1055 (1991); Phys. Rev. A **46**, 1922 (1992); Phys. Rev. A **46**, 1886 (1992); J. Low Temp. Phys. **89**, 145 (1992).
- [6] H. Li and M. Kardar, Phys. Rev. Lett. **67**, 3275 (1991); Phys. Rev. A **46**, 6490 (1992).
- [7] M. Krech, J. Phys. Condens. Matter **11**, R391 (1999).
- [8] U. Ritschel and M. Gerwinski, Physica (Amsterdam) **243A**, 362 (1997).
- [9] R. Garcia and M. H. W. Chan, Phys. Rev. Lett. **83**, 1187 (1999); Physica (Amsterdam) **280B**, 55 (2000).
- [10] R. J. Dionne and R. B. Hallock, in *Quantum Fluids and Solids—1989*, edited by Gary G. Ihas and Yasumasa Takano, AIP Conf. Proc. No. 194 (AIP, New York, 1989), p. 199.
- [11] A. Mukhopadhyay and B. M. Law, Phys. Rev. Lett. **83**, 772 (1999); Phys. Rev. E **62**, 5201 (2000).
- [12] G. Ahlers and D. S. Greywall, Phys. Rev. Lett. **29**, 849 (1972); H. A. Kierstead, J. Low Temp. Phys. **35**, 25 (1979); E. H. Graf, D. M. Lee, and J. D. Reppy, Phys. Rev. Lett. **19**, 417 (1967).
- [13] R. Garcia and M. H. W. Chan, J. Low Temp. Phys. **121**, 495 (2000).
- [14] M. W. Pestak and M. H. W. Chan, Phys. Rev. B **30**, 274 (1984).
- [15] J.-P. Laheurte, J.-P. Romagnan, and W. F. Saam, Phys. Rev. B **15**, 4214 (1977); J. Low Temp. Phys. **30**, 425 (1978).
- [16] G. Goellner, R. Behringer, and H. Meyer, J. Low Temp. Phys. **13**, 113 (1973); M. G. Ryschekewitsch and H. Meyer, J. Low Temp. Phys. **35**, 103 (1979); H. Meyer (private communication).
- [17] F. F. Harris-Lowe and K. A. Smee, Phys. Rev. A **2**, 158 (1970).
- [18] D. B. Crum, D. O. Edwards, and R. E. Sarwinski, Phys. Rev. A **9**, 1312 (1974).
- [19] I. E. Dzyaloshinskii, E. M. Lifshitz, and L. P. Pitaevskii, Adv. Phys. **10**, 165 (1961); E. Cheng and M. W. Cole, Phys. Rev. B **38**, 987 (1998); G. Vidali *et al.*, Surf. Sci. Rep. **12**, 133 (1991); S. Rauber *et al.*, Surf. Sci. **123**, 173 (1982).
- [20] H. A. Kierstead, J. Low Temp. Phys. **24**, 497 (1976).
- [21] M. E. Fisher, in *Critical Phenomena*, Proceedings of the 51st "Enrico Fermi" Summer School, Varenna, edited by M. Green (Academic, New York, 1971), p. 1; V. Privman and M. E. Fisher, Phys. Rev. B **30**, 322 (1984).
- [22] D. Ross, J. E. Rutledge, and P. Taborek, Phys. Rev. Lett. **76**, 2350 (1996).
- [23] M. Krech (private communication).
- [24] P. Leiderer, D. R. Watts, and W. W. Webb, Phys. Rev. Lett. **33**, 483 (1974).